

# Lawrence Berkeley National Laboratory

## Recent Work

### Title

NUCLEAR FISSION INDUCED BY RADIATIONLESS TRANSITIONS IN THE MU-MESONIC ATOMS Th232, U235, AND U238

### Permalink

<https://escholarship.org/uc/item/8jj2j1m8>

### Author

Diaz, Justo A.

### Publication Date

1962-05-09

UCRL 10214

University of California  
Ernest O. Lawrence  
Radiation Laboratory

TWO-WEEK LOAN COPY

*This is a Library Circulating Copy  
which may be borrowed for two weeks.  
For a personal retention copy, call  
Tech. Info. Division, Ext. 5545*

NUCLEAR FISSION INDUCED BY RADIATIONLESS  
TRANSITIONS IN THE MU-MESONIC ATOMS  
 $\text{Th}^{232}$ ,  $\text{U}^{235}$ , AND  $\text{U}^{238}$

Berkeley, California

## **DISCLAIMER**

This document was prepared as an account of work sponsored by the United States Government. While this document is believed to contain correct information, neither the United States Government nor any agency thereof, nor the Regents of the University of California, nor any of their employees, makes any warranty, express or implied, or assumes any legal responsibility for the accuracy, completeness, or usefulness of any information, apparatus, product, or process disclosed, or represents that its use would not infringe privately owned rights. Reference herein to any specific commercial product, process, or service by its trade name, trademark, manufacturer, or otherwise, does not necessarily constitute or imply its endorsement, recommendation, or favoring by the United States Government or any agency thereof, or the Regents of the University of California. The views and opinions of authors expressed herein do not necessarily state or reflect those of the United States Government or any agency thereof or the Regents of the University of California.

Research and Development

UCRL-10214

UNIVERSITY OF CALIFORNIA  
Lawrence Radiation Laboratory  
Berkeley, California  
Contract No. W-7405-eng-48

NUCLEAR FISSION INDUCED BY RADIATIONLESS TRANSITIONS IN  
THE MU-MESONIC ATOMS  $\text{Th}^{232}$ ,  $\text{U}^{235}$ , AND  $\text{U}^{238}$

Justo A. Diaz  
(Thesis)

May 9, 1962

NUCLEAR FISSION INDUCED BY RADIATIONLESS TRANSITIONS IN  
THE MU-MESONIC ATOMS  $\text{Th}^{232}$ ,  $\text{U}^{235}$ , AND  $\text{U}^{238}$

Contents

Abstract . . . . .	v
I. Introduction . . . . .	1
A. Review of $\mu$ -Meson Properties . . . . .	2
B. $\mu$ -Mesic Atoms . . . . .	4
II. Theory . . . . .	10
III. Experimental Method . . . . .	16
A. Electronics . . . . .	21
B. Beam . . . . .	24
C. Procedure for Taking Data . . . . .	25
IV. Data Analysis . . . . .	30
V. Discussion and Conclusions . . . . .	43
Acknowledgments . . . . .	48
Appendix . . . . .	49
References . . . . .	50

NUCLEAR FISSION INDUCED BY RADIATIONLESS TRANSITIONS IN  
THE MU-MESONIC ATOMS  $\text{Th}^{232}$ ,  $\text{U}^{235}$ , AND  $\text{U}^{238}$

Justo A. Diaz

Lawrence Radiation Laboratory  
University of California  
Berkeley, California

May 9, 1962

ABSTRACT

The time distribution of fissions in  $\text{Th}^{232}$ ,  $\text{U}^{235}$ , and  $\text{U}^{238}$  induced by  $\mu^-$  mesons was measured with a multiplate gas-scintillation fission chamber.

A significant number of prompt fissions that are not associated with  $\mu^-$  nuclear capture were observed. The results are:

<u>Nucleus</u>	<u>Ratio of prompt fissions to fissions from nuclear capture</u>
$\text{Th}^{232}$	$0.064 \pm 0.022$
$\text{U}^{238}$	$0.072 \pm 0.014$
$\text{U}^{235}$	$0.111 \pm 0.021$

The work of Mukhin et al. shows that the intensities of  $\mu$ -mesic K x rays for these elements relative to Pb are  $0.85 \pm 0.0$  ( $\text{Th}^{232}$ ),  $0.77 \pm 0.04$  ( $\text{U}^{238}$ ), and  $0.71 \pm 0.05$  ( $\text{U}^{235}$ ). This intensity reduction is qualitatively consistent with earlier predictions that, for these elements, a direct excitation of the nucleus competes with electromagnetic radiation in the transition to the ground state of the mesic atom. Our results indicate such direct nuclear excitation.

The number of fissions observed can be made quantitatively consistent with the results of Mukhin et al. and with photofission data when the effect on the fission barrier of the  $\mu$  meson in the 1S state of the mesic atom is taken into consideration.

## I. INTRODUCTION

When we take into consideration our knowledge of elementary particles, the  $\mu$  meson appears as a great puzzle. It has the same properties as the electron, when the properties are corrected for the  $\mu$ -meson mass: charge, spin, magnetic moment, and weak interaction; at the same time their masses are two orders of magnitude apart. As a result of this similarity an extensive study of the  $\mu$ -meson properties is being done. The weak interaction of the  $\mu$  meson is being studied to determine the form of the interaction through the process of  $\mu^-$  capture in hydrogen, and the effect of the hyperfine structure on the capture process in complex nuclei. The decay of  $\mu$  mesons in the process  $\mu^\pm \rightarrow e^\pm + \nu + \bar{\nu}$  has been studied extensively and the essential features of the interaction have been determined. Experiments are in progress to put upper limits on such expected  $\mu$  decay as  $\mu^\pm \rightarrow e^\pm + \gamma$  and  $\mu^\pm \rightarrow e^\pm + e^+ + e^-$ , but these decays have not been observed yet. The electromagnetic properties of the  $\mu$  meson are being studied through the determination of the magnetic moment,  $\mu$  scattering on complex nuclei, and the  $\mu$ -mesic atom.

The study of the  $\mu$ -mesic atom has shown that the x-ray yield in high-Z mesic atoms is lower than expected.<sup>1</sup> Zaretsky<sup>2</sup> in 1958 proposed that low-lying  $\mu$ -mesic atomic transition may induce nuclear excitation instead of emitting a photon. We have studied the time distribution of fission events associated with stopping  $\mu^-$  mesons in  $U^{238}$ ,  $U^{235}$ , and  $Th^{232}$  to determine if there are fission events that are not associated with  $\mu^-$  nuclear capture and to see if their timing is compatible with radiationless transitions. Before we proceed to the description of our experiment we present a review of the properties of the  $\mu$  meson.

## A. Review of $\mu$ -Meson Properties

### 1. The $\mu$ -meson weak interaction

#### a. Decay

The decay of the  $\mu$ -mesons is described by (a) the shape of the electron (positron) momentum spectrum, (b) the sign and magnitude of the asymmetry in the angular distribution of the electron (positron), (c) the polarization of the electron (positron), and (d) the decay lifetime.

The momentum and angular distribution of the emitted electron (positron) is given by<sup>3</sup>

$$\frac{dN}{dx d\Omega} \propto x^2 \left\{ 3(1-x) + 2\rho \left(\frac{4}{3}x - 1\right) \mp \xi \cos\theta \left[ 1 - x + 2\delta \left(\frac{4}{3}x - 1\right) \right] \right\},$$

where the mass of the electron has been neglected in comparison with its momentum  $x$ ; the  $\mp$  signs refer to  $\mu^-$  and  $\mu^+$  decay, respectively;  $\theta$  is the angle between the  $\mu$ -meson spin and the electron (positron) momentum; and  $x$  is the electron (positron) momentum in units of its maximum momentum  $m_\mu/2$ . The parameters  $\rho$ ,  $\delta$ , and  $\xi$  (the asymmetry parameter) are given in terms of the coupling constants. The two-component neutrino theory with a V-A interactions predicts  $\rho = 3/4$  and  $\xi = -1$ . The latest experimental results are:  $\rho = 0.77 \pm 0.042$ ,  $\delta = 0.782 \pm 0.031$  and  $P|\xi| = 0.848 \pm 0.036$ , where  $P$  is the  $\mu$ -meson polarization,<sup>4</sup> in agreement with the predictions of the two-component neutrino theory with a V-A interaction. The sign and magnitude of  $\xi$  can be determined experimentally when one knows the polarization and helicity of the decaying  $\mu$ -mesons. The helicity of the  $\mu^-$  meson has been determined to be positive,<sup>5</sup> thus  $\xi$  is negative, in agreement with V-A interaction.

The helicity of the electron (positron) emitted in the decay has been determined as being positive for positrons and negative for electrons,<sup>6</sup> again in agreement with the V-A type of interaction.

The lifetime of the  $\mu^+$  meson has been measured very accurately; the weighted mean of the results is  $\tau = 2.212 \pm 0.003$ .<sup>7</sup> This value is



in disagreement with the calculated value  $\tau = 2.31 \pm 0.05$ .<sup>8</sup>

b.  $\mu$ -meson capture

The  $\mu$ -meson capture is not as well understood as the  $\mu$ -meson decay, because of the lack of experimental knowledge of the elementary process  $\mu^- + p \rightarrow n + \text{neutrino}$ . The knowledge of  $\mu$ -meson capture is restricted essentially to the capture rates in complex nuclei.<sup>9</sup> Calculations based on a closure approximation<sup>10</sup> agree with the experimental results of Sens,<sup>9</sup> within the experimental and approximation errors. These calculations were made including in the weak-interaction Hamiltonian the induced pseudoscalar interaction<sup>11</sup> and weak magnetism<sup>12</sup> with coupling constants  $g_v^{(\mu)} = g_v^\beta \times 0.972$ ;  $g_a^{(\mu)} = g_a^\beta \times 0.999$ ;  $g_p^{(\mu)} = +8g_a^{(\mu)}$ . The other parameter of  $\mu$  capture, the asymmetry in the angular distribution of the emitted neutrons, has been measured but there is no agreement as to its absolute value. The experimental results are: Baker and Rubbia<sup>13</sup> found  $\alpha$  (the asymmetry parameter) to be positive and small ( $\alpha$  standard deviation from zero); measurements by Astbury et al.<sup>14</sup> obtained  $\alpha \approx -0.4$  (the actual experimental result is  $\alpha \phi P_\mu = -0.045 \pm 0.015$ , where  $\phi$  is a measure of the boil-off neutron contamination which is emitted isotropically and  $P_\mu$  is the  $\mu$ -meson polarization); and Telegdi et al.<sup>15</sup> obtained  $\alpha P_\mu = -0.020 \pm 0.005$  for neutrons and  $\alpha P_\mu = -0.022 \pm 0.004$  for electrons in Mg. Comparing these results one finds that  $\alpha$  for the neutrons is approximately equal to the  $\alpha$  for electrons (for electrons,  $\alpha = -0.33$ ) in magnitude and sign.

The latest development is the evidence for the relative phase of the Fermi and Gamow-Teller part of the interaction from studies of the hyperfine effect in F<sup>19</sup> that points to F - GT theory.<sup>16</sup> Also, the first results of  $\mu^-$  capture in liquid hydrogen are available, with preliminary results again pointing to V-A theory.<sup>17</sup>

2. The  $\mu$ -meson electromagnetic interaction

The electromagnetic interaction of  $\mu$  mesons has been studied through (a) the measurement of the magnetic moment ( $g-2$  experiment), (b) the scattering of  $\mu$  mesons on complex nuclei, and (c)  $\mu$ -mesic atoms.

The  $\mu$ -meson magnetic moment has been measured<sup>18</sup> to order  $\frac{\alpha}{2\pi}$ , giving  $\frac{g-2}{2} = 0.001145 \pm 0.000022$ . At present there are experiments in progress at Berkeley by Schrank et al.<sup>19</sup> to measure the magnetic moment to order  $(\frac{\alpha}{2\pi})^2$ . The measurements reported show no disagreement with the value predicted by electrodynamics,  $\frac{g-2}{2} = 0.001165$ .

The scattering of  $\mu$  mesons on complex nuclei has been a source of controversy, with some cosmic-ray experiments yielding an anomalous cross section at large angles when compared with the coulomb-scattering cross section.<sup>20</sup> The latest experiment by Masek et al.<sup>21</sup> shows no deviation from the calculated coulomb-scattering values up to a momentum transfer of 600 MeV/c

#### B. $\mu$ -Mesic Atoms

The formation of  $\mu$ -mesic atoms was first deduced from the  $\mu$ -meson decay rates:<sup>22</sup>  $\mu$ -mesons were observed to decay when stopped in light elements but not in heavy elements. Wheeler<sup>23</sup> calculated the capture rates of bound  $\mu$ -mesons in a 1S state and showed that the capture rate would vary as  $Z^4$ .

The  $Z^4$  dependence of the capture rate can be obtained as follows if one assumes a point nucleus: Let  $\psi(r)$  be the  $\mu$ -meson wave function in the 1S state, where  $r$  is the distance from the nucleus. The probability of finding the  $\mu$  meson at the nucleus is given by  $|\psi(r)|^2$ , evaluated at  $r = 0$ . There are  $Z$  protons in the nucleus, all having the same probability of capturing the  $\mu$  meson. The capture rate is then proportional to

$$\Lambda_{\text{cap}} \propto Z |\psi(0)|^2.$$

For the 1S state  $\psi(r) = 2 \left( \frac{Z}{a_\mu} \right)^{3/2} \exp(-Zr/a_\mu)$ ,

where  $a_\mu$  is the  $\mu$ -meson Bohr radius. Then

$$\Lambda_{\text{cap}} \propto Z \left( \frac{Z}{a_\mu} \right)^3 \text{ or } \Lambda_{\text{cap}} \propto Z^4.$$

Ticho,<sup>24</sup> from the measurements of the decay rates in light nuclei, deduced that the capture rate varies as  $Z^{3.7 \pm .85}$ ; this is the first experimental evidence of  $\mu$ -mesic atoms. The first observation of  $\mu$ -mesic x rays was obtained in carbon by Butement,<sup>25</sup> who found a peak at an energy of 80 keV—the energy of the  $\mu^- K_{\alpha}$  x ray in that element.

When the  $\mu$  meson is in a Bohr orbit with principal quantum number  $n = 14$ , it is already inside the electronic K shell. The  $\mu$ -meson Bohr radius is smaller than the electron Bohr radius in the ratio of  $m_e/m_{\mu} = 1/207$  for large  $n$  orbits. The energy levels are calculated accurately with hydrogenic wave functions in low- $Z$  elements. The closeness of the  $\mu$  meson to the nucleus for high- $Z$  elements makes it necessary to take into consideration the  $\mu$ -meson wave-function overlap with the nuclear volume. The potential binding the  $\mu$ -meson is no longer a pure Coulomb potential, but if one assumes a uniform charge distribution of radius  $R$  for the nucleus, the potential has the form

$$V = -\frac{Ze^2}{r} \quad | r > R,$$
$$V = \frac{Ze^2}{R} \cdot (3/2 - 1/2 r^2/R^2) \quad | r < R, \quad (1)$$

where

$r$  = distance of the  $\mu$  meson from the center of the nucleus.

This potential form lowers the binding energy of the low-lying states of the  $\mu$ -mesic atoms.

The measurement of  $\mu$ -mesic x-ray energies has been done using sodium iodide crystals and proportional counters. The measured energies agree with the calculated values when the finite nuclear size in large- $Z$  nuclei is taken into consideration. Table I shows the measured and calculated energies for different elements.

Table I. Comparison of theoretical and experimental values of the 2P-1S transition energy in  $\mu$ -mesic atoms.

Element	Z	Experimental 2P-1S transition energy <sup>a</sup>	Theoretical 2P-1S <sub>b</sub> transition energy
Al	13	0.35	0.3443
Si	14	0.41	0.3970
Ti	22	0.955	0.9198
Mn	25	1.55	1.4965
Cu	29	1.60	1.5865
Sb	51	3.50	3.5283
Pb	82	6.02	5.9620

<sup>a</sup>See reference 26.

<sup>b</sup>See reference 27.

The 2P-1S transition energy for high-Z mesic atoms is very sensitive to the radius of the nuclear charge distribution. Fitch and Rainwater,<sup>26</sup> and Hill and Ford<sup>28</sup> calculated the radius of a spherically symmetric uniform charge distribution to fit the data of Fitch and Rainwater and found the radius to vary as  $r^0 \times A^{1/3}$ , where  $r^0 = 1.20 \times 10^{-13}$  cm—in good agreement with the value later obtained from electron-scattering experiments. Also, the transition energy allows an accurate measurement of the  $\mu$ -meson mass in elements where the nuclear charge can be considered a point charge. A measurement of the transition energy of the  $3D_{5/2} - 2P_{3/2}$  transition in phosphorous by the critical absorption of the x ray in Pb yields<sup>29</sup>

$$\frac{m_{\mu}}{m_e} = 206.78 \begin{matrix} +0.03 \\ -0.02 \end{matrix} .$$

Measurements of the x-ray yield from  $\mu$ -mesic atoms have been carried out by Stearns and Stearns<sup>1</sup> and Lathrop et al.<sup>1</sup> in the region of low-Z nuclei, and by Mukhin et al.<sup>1</sup> and Hincks et al.<sup>1</sup> in the high-Z region. All measurements were made with NaI crystals. The results of Stearns and Stearns showed a very low yield for the K x-ray series in Li, Be, B, C, and N. The work of Lathrop et al. in the same elements shows that the x-ray yield is 100% as expected with the exception of Li whose yield is 53%. (See Table II for the results of these experiments.)

The results of Stearns and Stearns are not substantiated by the measurement by Lathrop et al. The only apparent difference between the two experiments is the resolution time of the coincidence between the  $\mu$ -meson stop signal and the x ray detected in the NaI(Tl) crystal:  $5 \times 10^{-8}$  sec in the Stearns and Stearns experiment, and  $10^{-7}$  sec in the Lathrop et al. experiment. Stearns and Stearns clipped the NaI crystal photomultiplier pulse (they used a Dumond 6292 photomultiplier) to  $2.5 \times 10^{-8}$  sec to perform the fast coincidence. In the case of a 30-keV x ray, with this clipping time, from the number of photons emitted by the crystal and from the quantum efficiency of the photocathode of the Dumond 6292 photomultiplier, one would expect approximately seven photoelectrons into the first dynode. Fluctuations in this number of photoelectrons will induce considerable time jitter in the pulse, with subsequent loss of coincidences and a decrease in the apparent x-ray yield. From the report of the experiment one does not know the minimum number of photons that could be detected. As a result one cannot draw any quantitative conclusions as to the reduction of the x-ray yield due to statistical fluctuation in the number of photoelectrons into the first dynode.

Table II. Measured K x-ray yield in low-Z  $\mu$ -mesic atoms.

Element	K x-ray yield	
	Stearns and Stearns <sup>a</sup>	Lathrop et al. <sup>a</sup>
Li	< 0.16	0.53 ± 0.05
Be	0.33 ± 0.03	1.01 ± 0.10
B	0.46 ± 0.035	1.12 ± 0.17
C	0.60 ± 0.04	0.97 ± 0.10
N	0.82 ± 0.07	1.01 ± 0.10
O	0.80 ± 0.05	1.01 ± 0.10

<sup>a</sup> See reference I.

Fermi and Teller<sup>30</sup> showed that the time necessary for a  $\mu$  meson to lose energy from 2 keV and be captured in a mesic atom is of the order of  $10^{-13}$  sec. The calculations of Burbidge and de Borde<sup>31</sup> show that the cascading process of the  $\mu$  meson to the 1S state in a mesic atom, considering Auger and radiative transitions, is of the order of  $10^{-14}$  sec. Ruderman<sup>32</sup> has shown that there exist no recognized theoretical reasons for low x-ray yield in low-Z mesic atoms.

In the high-Z mesic atoms Th<sup>232</sup>, U<sup>238</sup>, and U<sup>235</sup> the K x-ray yield is also low. Table III shows the results of Mukhin et al.<sup>1</sup> and Hincks et al.<sup>1</sup> Prior to this experiment it was suggested by Zaretsky<sup>2</sup> that  $\mu$ -mesic 2P-1S transitions may transfer the quantum of energy directly to the nucleus (see Sec. II for a more detailed description of the mechanism). The energy of 2P-1S transition is approximately 6.3 MeV in the elements showing the low x-ray yield. This energy is higher than the neutron binding energy and the measured fission thresholds of these elements. (See Table IV for these data.)

In our experiment we find evidence for the mechanism proposed by Zaretsky. The presence of nuclear excitation not associated with  $\mu$  nuclear capture has been detected, and the results are explained by the radiationless transition, although we are not able to account directly for all the missing x rays. By comparing our results with photonuclear excitation data we conclude that the  $\mu$  meson in a 1S state increases the fission threshold, thus reducing the fission probability of the excited nuclei.

Table III. Measured 2P-1S x-ray yield relative to Pb in high-Z  $\mu$ -mesic atoms.

Element	2P-1S transition x-ray yield	
	Mukhin et al. <sup>a</sup>	Hincks et al. <sup>a</sup>
W		1.05 ± 0.1
Pb	1	1
Bi	1 ± 0.06	0.9 ± 0.1
Th <sup>232</sup>	0.85 ± 0.0	
U <sup>238</sup>	0.77 ± 0.04	0.7 ± 0.1
U <sup>235</sup>	0.71 ± 0.05	

<sup>a</sup> See reference 1.

Table IV. Neutron binding energy and fission threshold in U<sup>238</sup>, U<sup>235</sup>, and Th<sup>232</sup>

Element	Neutron binding energy <sup>a</sup>	Measured fission threshold <sup>b</sup>	Estimated fission barrier <sup>c</sup>
U <sup>238</sup>	6.03 ± .13	5.8 ± .15	5.80
U <sup>235</sup>	5.37 ± .15	5.31 ± .25	5.75
Th <sup>232</sup>	6.20 ± .04	5.40 ± .22	5.95

<sup>a</sup> See reference 33.

<sup>b</sup> See reference 34.

<sup>c</sup> See reference 35.

## II. THEORY

In this section we shall present an outline of Zaretsky and Novikov's<sup>36</sup> calculations of the ratio of radiationless transition to x-ray emission probabilities in the 2P-1S transition in  $\mu$ -mesic atoms.

The mean radius of the 2P state in a mesic atom is of the order of  $10^{-10}/Z$  cm. For high-Z atoms -  $Z \approx 90$  - the  $\mu$  mesons spends a large fraction of the time inside of the nucleus. The 2P-1S transition may induce nuclear excitation by a similar mechanism to an inverse internal conversion. In internal conversion in nuclear physics an excited nucleus transfers part or all of its excitation energy to one of the orbital electrons, usually a K-orbit electron that is ejected from the atom, and by inverse internal conversion we mean that the  $\mu$  meson in its transition from the 2P to the 1S state transfers the quantum of energy to the nucleus. Radiationless transition of this type would be expected with measurable probability when  $\rho\Gamma_{re} \gg 1$ , where  $\rho$  is the nuclear level density at the 2P-1S transition energy and  $\Gamma_{re}$  is the energy width of the radiationless transition.

We proceed now to an outline of the calculation of  $\Gamma_{re}/\Gamma_{\gamma}$ , where  $\Gamma_{\gamma}$  is the width for x-ray emission in the 2P-1S transition.

The 2P-1S transition is an electric-dipole transition, and the level width for x-ray emission is given by

$$\Gamma_{\gamma} = \frac{4}{9} e^2 \omega^3 / c^3 \left| \int_0^{\infty} R_{2P} r R_{1S} r^2 dr \right|^2, \quad (2)$$

where  $R_{1S}$  and  $R_{2P}$  are the radial wave functions of the 1S and 2P states and  $\omega$  is the energy of 2P-1S transition.

The integral is

$$\int_0^{\infty} r^3 R_{1S} R_{2P} dr = \frac{Ze^2}{m_{\mu}\omega^2} f(R),$$



where

$$f(R) = \frac{1}{R^3} \int_0^R r^3 R_{1S} R_{2P} dr + \int_R^\infty R_{1S} R_{2P} dr,$$

when the potential for the  $\mu$  meson is of the form described by Eq. (1) in the introduction, with  $R$  being the nuclear radius.

For the radiationless transition the Coulomb interaction potential between the nucleus and the  $\mu$  meson is given by

$$V = -\frac{4}{3} \pi e^2 \sum_{i=1}^Z \sum_{m'} Y_{1m'}(\theta_i) Y_{1m'}^*(\theta_\mu) \times \begin{cases} r_i/r_\mu^2 & \text{for } r_\mu \geq r_i \\ r_\mu/r_i^2 & \text{for } r_\mu \leq r_i, \end{cases}$$

where  $\theta_i$ ,  $r_i$ ,  $\theta_\mu$ , and  $r_\mu$  are, respectively, the coordinates of the  $i$ th proton and the  $\mu$  meson. This potential is the dipole term in the expansion of the potential  $e^2/|r_i - r_\mu|$  that is determined by the 2P-1S transition being an electric-dipole transition.

Let us consider a  $\mu$ -mesic atom with spin-0 nucleus. The wave function describing the muon in the 2P state and the nucleus in its ground state is  $\psi_i = \psi_0 R_{2P} Y_{1m}(\theta_\mu)$ , where  $\psi_0$  is the nuclear ground-state wave function. The final state is described by  $\psi_f = \psi_{1m} R_{1S}/4\pi$ , where  $\psi_{1m}$  is the wave function of a nucleus with spin 1 and magnetic quantum number  $m$  and an excitation energy  $E_{2P-1S}$ . The matrix element for the transition is

$$\langle \psi_f | V | \psi_i \rangle = \frac{2}{3} \pi^{1/2} e^2 \langle \psi_{1m} | \sum_{i=1}^Z r_i Y_{1m}(\theta_i) f(r_i) | \psi_0 \rangle \delta_{mm'},$$

where

$$f(r_i) = \frac{1}{r_i^3} \int_0^{r_i} r^3 R_{1S} R_{2P} dr + \int_{r_i}^\infty R_{1S} R_{2P} dr,$$

and

$$f(r_i) \text{ is } f(R) \text{ for } r_i = R.$$

Then the radiationless-transition-level width is given by

$$\Gamma_{re} = \frac{8}{9} \pi^2 e^4 \left| \langle \psi_{1m} \left| \sum_{i=1}^Z r_i Y_{1m}(\theta_i) f(r_i) \right| \psi_0 \rangle \right|_{av}^2 \rho, \quad (3)$$

where  $\rho$  is the nuclear level density of final states, and the nuclear matrix element has been averaged over initial and final states.

Taking the ratio  $\Gamma_{re} / \Gamma_{\gamma}$  we have

$$\frac{\Gamma_{re}}{\Gamma_{\gamma}} = 2 \pi^2 \left( \frac{m_{\mu} c^2}{Z} \right)^2 \frac{\omega}{e^2 c} \left| \langle \psi_1 \left| \sum_{i=1}^Z r_i Y_{1m}(\theta_i) \frac{f(r_i)}{f(R)} \right| \psi_0 \rangle \right|_{av}^2 \rho.$$

Now the nuclear photoexcitation cross section is given by

$$\sigma = \frac{16}{3} \pi^3 \frac{\omega}{c} e^2 \left| \langle \psi_1 \left| \sum_{i=1}^Z r_i Y_{1m}(\theta_i) \right| \psi_0 \rangle \right|_{av}^2 \rho. \quad (4)$$

Substituting in  $\frac{\Gamma_{re}}{\Gamma_{\gamma}}$  we have

$$\frac{\Gamma_{re}}{\Gamma_{\gamma}} = \frac{3}{8\pi} \left( \frac{m_{\mu} c^2}{Z e^2} \right)^2 \sigma B, \quad (5)$$

where

$$B = \frac{|\langle \psi_1 | \sum_i r_i Y_{1m}(\theta_i) f(r_i) | \psi_0 \rangle|_{av}^2}{|\langle \psi_1 | \sum_i r_i Y_{1m}(\theta_i) f(R) | \psi_0 \rangle|_{av}^2}.$$

For  $U^{238}$   $B = 1.8$ . This estimate is based on arguments for the behavior of the matrix elements given in reference 36.

The photoexcitation cross section  $\sigma$  can be estimated as follows: the photofission cross section<sup>37</sup> at 6.5 MeV is 12 mb in  $U^{238}$  and the ratio  $\frac{\sigma_f}{\sigma_f + \sigma_n} \approx 0.25$ , where  $\sigma_f$  is the photofission cross section and  $\sigma_n$  is the neutron emission cross section.<sup>38</sup>

The photoexcitation cross section is  $\sigma_n + \sigma_f$ , thus

$$\sigma = \sigma_n + \sigma_f = \sigma_f / 0.25 \approx 50 \text{ mb.}$$

Then, from Eq. (5),

$$\frac{\Gamma_{re}}{\Gamma_\gamma} = 0.70.$$

We can compare these results with the ratio obtained from the x-ray yield measurement—assuming that all the x-rays missing are due to this process:

$$\frac{\Gamma_{re}}{\Gamma_\gamma} \approx 0.30.$$

The theoretical value is about a factor of two from the experimental one. This indicates that the mechanism described by the calculation is a reasonable means of accounting for the low x-ray yield and for the nuclear excitation detected in the experiment being reported.

Let us consider qualitatively the behavior of  $\Gamma_{re}$  with A;  $\Gamma_{re}$  is proportional to the nuclear level density at the 2P-1S transition energy. The general trend of the nuclear level density is given by<sup>39</sup>

$$\frac{1}{\rho} = 4.1 \times 10^6 (\chi^4 e^{-\chi}) \quad (6)$$

where

$$\chi = \pi \left( \frac{AE}{E_f} \right)^{1/2},$$

and E is the excitation energy and  $E_f$  is the mean Fermi energy of the protons and neutrons.

From Eq. (6) we can see that  $\rho$  decreases, for the elements with which we are concerned, as A and E decrease with an expected decrease in  $\Gamma_{re}$ . Equation (6), while it does describe the general trend of the level density as a function of A, does not describe the level density near closed-shell nuclei. For example, the nuclear level density obtained from slow-neutron capture is  $10^{-4}$  as large in elements near Pb as the density predicted by Eq. (6). We also know that the 2P-1S transition energy decreases

approximately as  $Z^2$ , and as a result the radiationless-transition nuclear excitation will also decrease, again with an effective decrease in level density. On this basis one would expect radiationless transition to have a measurable probability in elements of high  $Z$  far from a closed shell.

For a more detailed discussion of these calculations, see reference 36.

### III. EXPERIMENTAL METHOD

The 2P-1S transition energy in  $\text{Th}^{232}$ ,  $\text{U}^{238}$ , and  $\text{U}^{235}$  is higher than the measured fission threshold. In  $\text{U}^{235}$  and  $\text{U}^{238}$  this transition energy is higher than the neutron binding energy, and both neutron emission and fission will occur. In  $\text{Th}^{232}$  the neutron binding energy is very close to the 2P-1S transition energy, and one may expect no neutron emission from the radiationless transition; in this case only fission, or possibly  $\gamma$  emission, will occur.

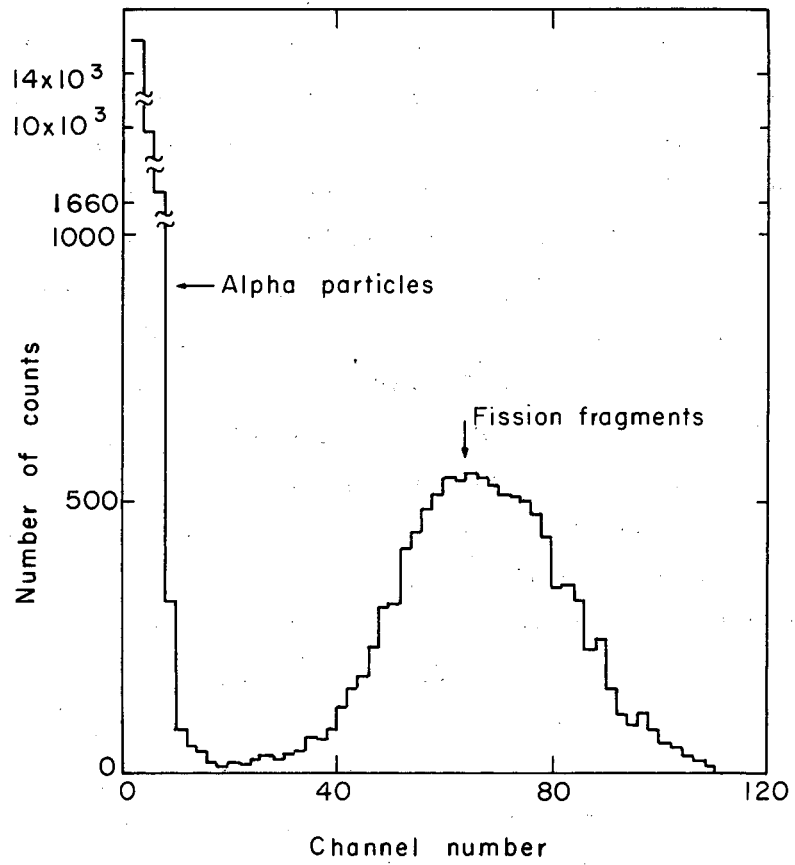
One may detect the radiationless transition nuclear excitation by the prompt neutron emission associated with it. These neutrons may have kinetic energy up to the difference of the 2P-1S transition energy and the neutron binding energy, giving approximately 0.9 MeV in  $\text{U}^{235}$ , 0.3 MeV in  $\text{U}^{238}$ , and less than 0.1 MeV in  $\text{Th}^{232}$ . It is necessary to separate these neutrons from neutrons due to  $\mu^-$ -capture nuclear excitation, for which the average neutron emission in lead, for example, is approximately 1.6 neutrons/ $\mu$  capture.<sup>40</sup> Time-of-flight technique has been used by Hincks et al.<sup>41</sup> in an attempt to detect the prompt neutrons. In this case one has to separate the neutrons produced by  $\mu$  capture, which means that energetic neutrons emitted at a later time have to be separated from slow prompt neutrons. This effect makes the data analysis for the experiment very difficult when one considers that the energy spectrum of neutrons emitted due to  $\mu^-$ -capture nuclear excitation is not known.

For this reason the present experiment was directed toward the fission process. As mentioned in Sec. IB, the 2P-1S transition is higher than the measured fission threshold in  $\text{Th}^{232}$ ,  $\text{U}^{238}$ , and  $\text{U}^{235}$ . From photofission data (see Sec. V for a detailed discussion) one may expect a large fraction of the nuclei excited by radiationless transition to undergo fission. The problems of detecting the prompt fission are reduced essentially by developing a fission detector with good time resolution, of the order of 3 nsec. For this purpose we developed a multiplate noble-gas scintillation chamber. The scintillator was a

mixture of 80% argon and 20% nitrogen; the nitrogen acted as a wavelength shifter.<sup>42</sup> In the present experiment all three targets were  $\alpha$ -particle emitters, so one had to discriminate against a large  $\alpha$  background. The chamber was operated at 45 psi; this made all fission fragments emerging from the targets stop in the gas. The fission-to- $\alpha$ -particle pulse height was at a ratio of better than 3:1 for a thin (a few  $\mu\text{g}/\text{cm}^2$ )  $\text{Cf}^{252}$  source. Figure 1a shows the  $\alpha$  and fission pulse height from  $\text{Cf}^{252}$ . The  $\alpha$  background was eliminated by pulse-height discrimination (see Sec. IIIA). Figure 1b shows the same pulse-height spectrum as in Fig. 1a discriminating against  $\alpha$  particles. With a thin  $\text{Cf}^{252}$  source the efficiency for detecting fissions in the chamber was approximately 100% when compared with a continuous-flow methane ionization chamber. Figure 2 is a photograph of the chamber. The chamber was viewed with two RCA 6655A photomultiplier tubes.

The targets of  $\text{Th}^{232}$  and  $\text{U}^{238}$  consisted of nine plates 3.25 in. in diameter. The  $\text{U}^{238}$  plates were 0.010 in. thick and the  $\text{Th}^{232}$  plates were 0.025 in. thick. However, due to the short range of the fission fragments, the effective target thickness for detecting a fission was very small. For  $\text{U}^{235}$  the target consisted of nine stainless steel plates 0.010 in. thick on which 1  $\text{mg}/\text{cm}^2$  of  $\text{U}^{235}\text{F}_4$  was evaporated on each side of all plates. The plates were polished and aluminized to maximize their reflectivity for better light-collection efficiency.

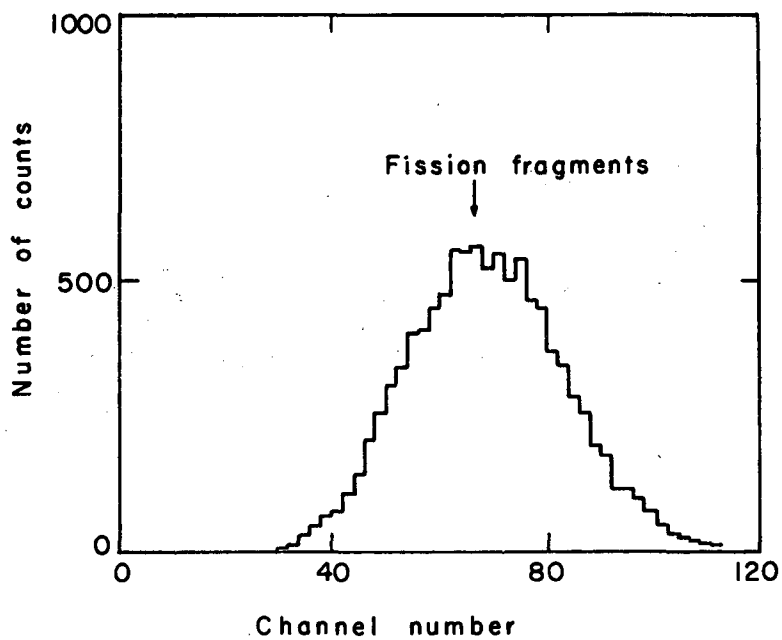
In order to separate the prompt fissions from  $\mu$ -capture fissions we measured the time distribution of the fissions relative to the muons stopped. Fissions from the radiationless transition have effectively a  $\delta$ -function distribution at zero time, and fissions from  $\mu$  capture have an exponential distribution characterized by the mean life of the muon in the target element. From a least-squares fit to the data, leaving out the first 10 nsec, one obtains the mean life and zero-time intercept that allows one to calculate the contribution of  $\mu$ -capture fissions in the first 10 nsec. The difference between the experimental number and the calculated one in the first 10 nsec is taken to be the contribution from radiationless transitions or any other prompt effect.



MU-27146

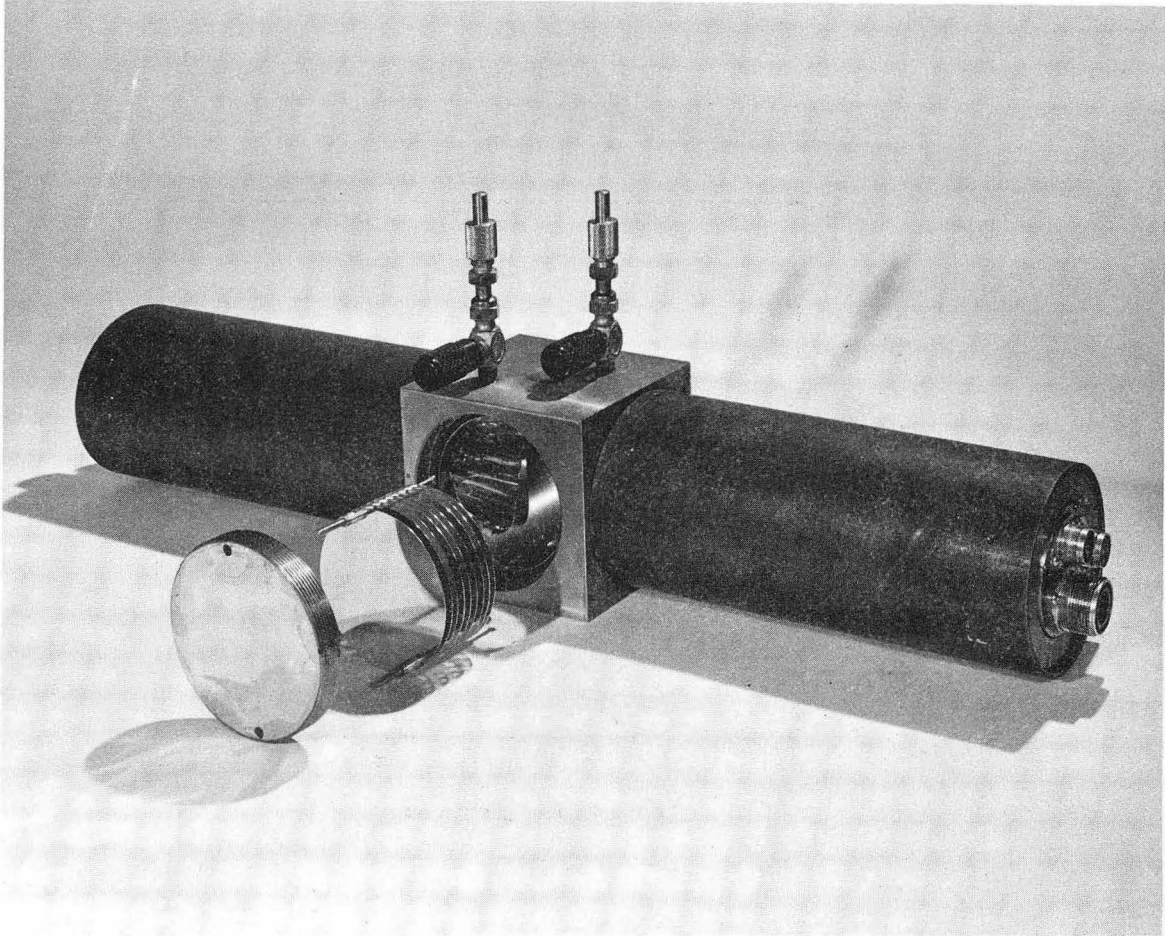
Fig. 1a. Alpha particles and fission fragments of Cf<sup>252</sup>: pulse-height distribution.





MU-27147

Fig. 1b. Fission fragments of  $\text{Cf}^{252}$ : pulse-height distribution after eliminating  $\alpha$ -particle pulses by pulse-height discrimination.



ZN-3123

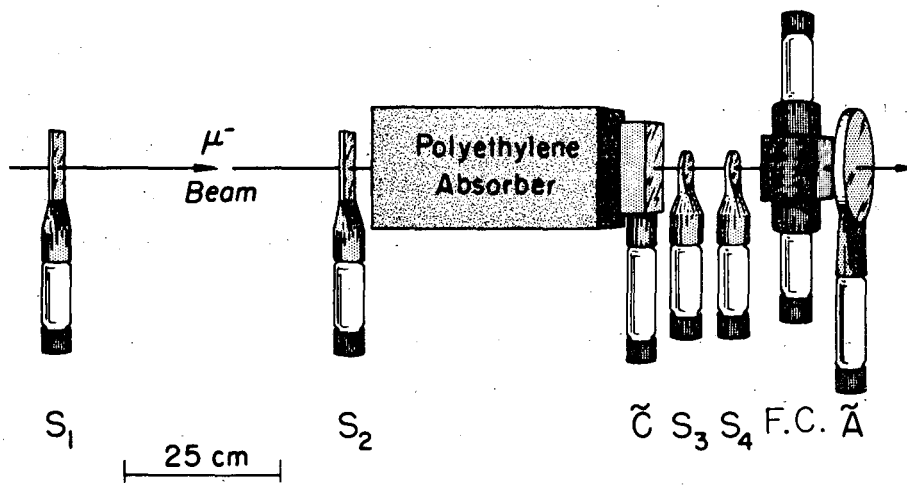
Fig. 2. The fission chamber, with a nine-plate target and the thin window for the  $\mu^-$  beam.

### A. Electronics

The counter telescope is shown in Fig. 3. All counters were made of plastic scintillator with the exception of the fission chamber (described previously) and counter C. This counter was a 5 by 5 by 1-in. water Cerenkov counter in a 0.125-in. -thick Lucite box to eliminate coincidences produced by electrons in the beam. Counters  $S_1$ ,  $S_2$ ,  $S_3$ , and  $S_4$  were viewed with RCA 6655A photomultiplier tubes, and counters C and A with RCA 6810A phototubes.

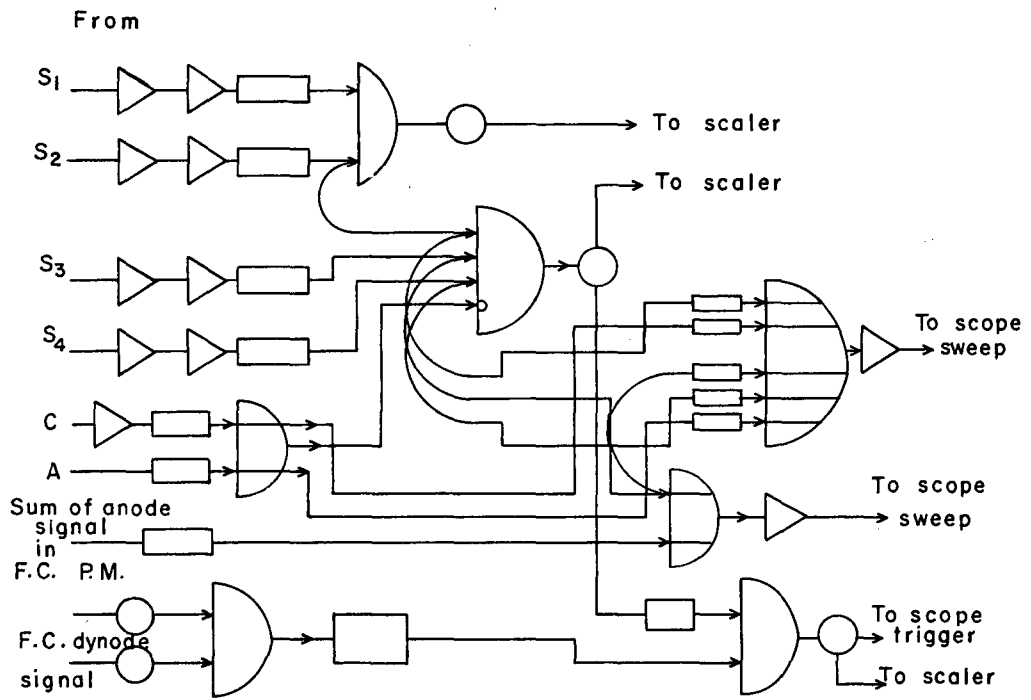
The beam monitor consisted of counters  $S_1$  and  $S_2$  in coincidence. The  $\mu^-$  stopping signal was a coincidence between counters  $S_3$  and  $S_4$  with the sum of counters A and C in anticoincidence. There were two outputs from each of the photomultiplier tubes looking at the fission chamber. The last dynode signal was fed into a 10-Mc discriminator. The discriminator was set so that the pulses produced by the  $\alpha$  particles from the counter did not get through. The fast output from the discriminators was set in coincidence. The output of this coincidence triggered a 0.5- $\mu$ sec gate that was set in coincidence with the delayed  $\mu^-$  stopping signal. The  $\mu^-$  stopping signal was delayed in such a way that, for zero-time fission gates, it arrived at the middle of the 0.5- $\mu$ sec gate. This allows us to measure the background at negative time, and study the effect of the time resolution on the time distribution of zero-time fissions. The signal from the anode of the fission chamber's photomultiplier was added at the base of the tube.

The output of the coincidence between the gate generated by the fission signal and  $\mu^-$  stopping signal was used to trigger a four-gun scope. The output of counters  $S_2$ , C,  $S_3$ ,  $S_4$ , and A were fed into an adder, which was timed in such a way that when the output of the adder was displayed in one of the scope sweeps there were at least 30 nsec between the pulses. In another scope sweep, counter  $S_3$  and the sum of the two photomultipliers of the fission chamber were displayed, timed in such a way that there were 100 nsec between  $S_3$  and the zero-time fissions. Both scope sweeps were time-calibrated by using a 50-Mc Tektronix crystal oscillator. A block diagram of the electronics is shown in Fig. 4.



MU-17654-A

Fig. 3. The counter telescope.



MU-27148

Fig. 4. Electronics block diagram.

## B. Beam

For this experiment a  $\mu$  beam of high purity was necessary, since fissions from  $\pi^-$ 's stopping in the targets have effectively the same time distribution as the fissions produced by radiationless-transition excitation. For experimental purposes this time distribution is a  $\delta$  function at zero time. The usual procedure to eliminate  $\pi^-$ 's is to tune the beam for a given momentum and maximize the beam flux with the cyclotron target position. (The  $\pi$  to  $\mu$  peak ratio under these conditions is usually 7:1.) Then the bending magnets in the beam are set for a momentum 10 to 15% higher than the momentum for which the cyclotron target position was maximized. This in general reduces the  $\pi$  to  $\mu$  peak ratio to 1:3 and, with slight adjustments in the cyclotron target position, this ratio can be reduced to 1:5 or better, and in many cases will eliminate the  $\pi$  almost completely if initial momentum spread is of the order of, or less than, 2%. This method is based on the fact that the  $\pi^-$  source for the beam is essentially a point source and has a maximum intensity when the beam is taken at 0 deg relative to the proton beam striking the target. The  $\mu$ -meson source produced by the decay of  $\pi^-$  near the target is a diffuse source and is not as anisotropic as the  $\pi^-$  source. Therefore, by detuning the magnet system after it has been focused on the cyclotron target, one changes the apparent source position to the neighborhood of the target. The  $\pi^-$ 's that have the larger momentum then have to be produced at larger angles, thus reducing the  $\pi^-$  yield.<sup>43</sup> At the same time the  $\mu^-$  yield is also reduced.

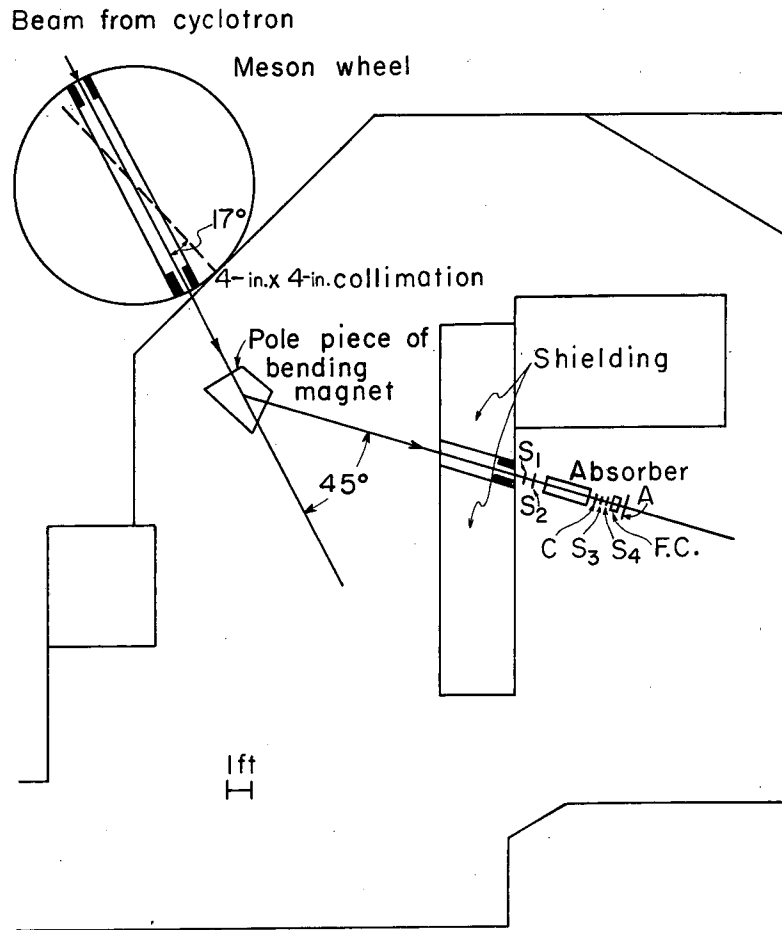
In this experiment, due to the small effective target thickness, the largest  $\mu$  yield was necessary. We separated the  $\pi^-$  and  $\mu^-$  by range (using a  $213 \pm 5$  MeV/c beam from the Berkeley 184-inch cyclotron). The  $\pi^-$  to  $\mu^-$  ratio in the beam was 5:1. The electrons were eliminated by use of the Cerenkov counter C, as described in the preceding section. The beam from the cyclotron was taken out through the meson wheel, collimated at the entrance and exit of the wheel to a 4-by 4-in. area, then bent 45 deg and collimated again to a 4-by 4-in. area before entering the experimental area. The magnet, with 28-deg-wedge pole pieces,

gave a momentum focus at the center of the absorber between counters  $S_2$  and C, and with sufficient dispersion to have a momentum spread of 2.5%. Figure 5 shows the experimental arrangement. In Fig. 6 we have a differential range curve with the  $\pi^-$  peak at 8-in. of  $CH_2$  and the  $\mu^-$  peak at 12.75 in. of  $CH_2$  (using a nine-plate stainless steel target). The targets were run at 12.5 in. of  $CH_2$ , since the average thickness of the actual targets was a little greater than the stainless steel. The  $\mu^-$  stopping rate in a 3.4-g/cm<sup>2</sup> target in an area defined by a 1.5-in. -diam counter was 20,000/min.

To estimate the  $\pi^-$  contamination we have to know the behavior of the high-energy side of the  $\pi^-$  peak in the range curve, since we have a momentum spread of 0.10R, while<sup>44</sup> for a monochromatic beam  $\frac{\sqrt{\Delta R^2}}{R} = 0.03$ . For this purpose we measured the prompt-fission yield as a function of absorber thickness near the  $\pi^-$  peak. The results are given in Fig. 7. The fission yield was fitted with a gaussian curve; we obtained  $P(\chi^2) \approx 0.50$ , which shows that the data is well-described by such a function. The  $\pi^-$  contamination was obtained by extrapolating this curve to 12.5 in. of  $CH_2$ , giving a ratio  $\pi^-/\mu^-$  of  $\approx 10^{-5}$ . As a further check we extrapolated the high-energy side of the range curve exponentially with absorber thickness to 12.5 in. of  $CH_2$ , yielding a ratio  $\pi^-/\mu^-$  of  $10^{-3}$ . We assume this number ( $10^{-3}$ ) to be the upper limit to the  $\pi^-$  contamination. In Sec. V we show that even if for some reason these estimates are in error the observed prompt fissions cannot possibly be explained by  $\pi^-$  contamination.

### C. Procedure for Taking Data

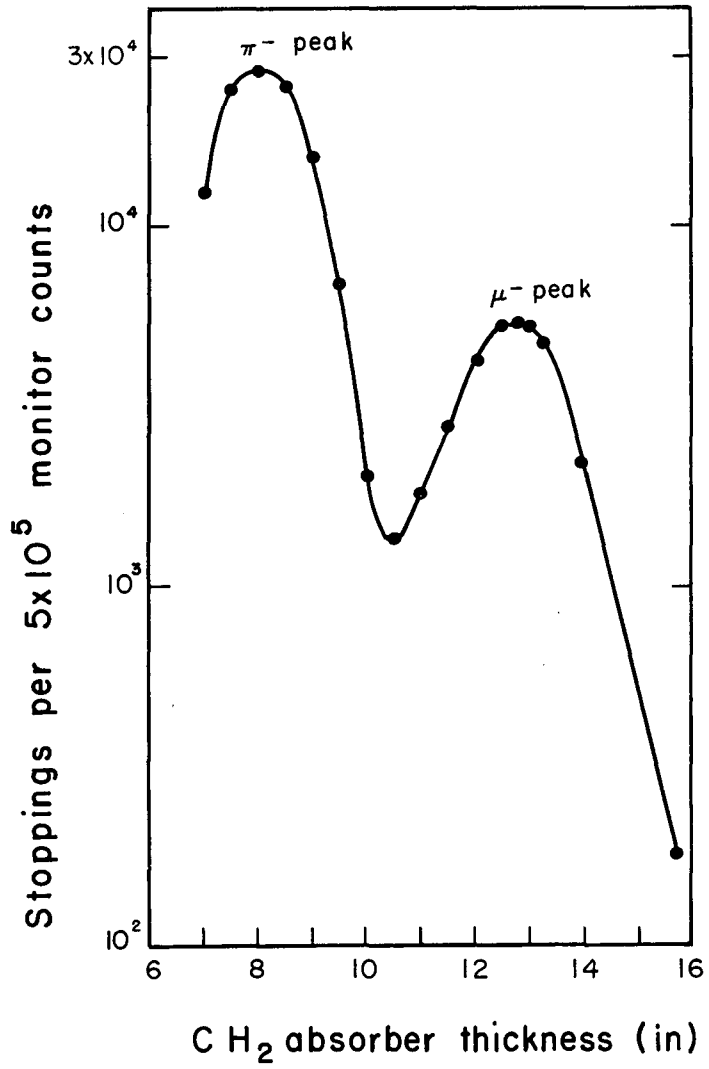
1. The differential range curve of the beam was determined every 48 h to determine the absorber depth at which to run the target, and to make estimates of the  $\pi$  contamination. The  $\mu$  stopping rate was checked after every target change, and a running check of the stopping rate per beam monitor was kept throughout the run.



MU-27151

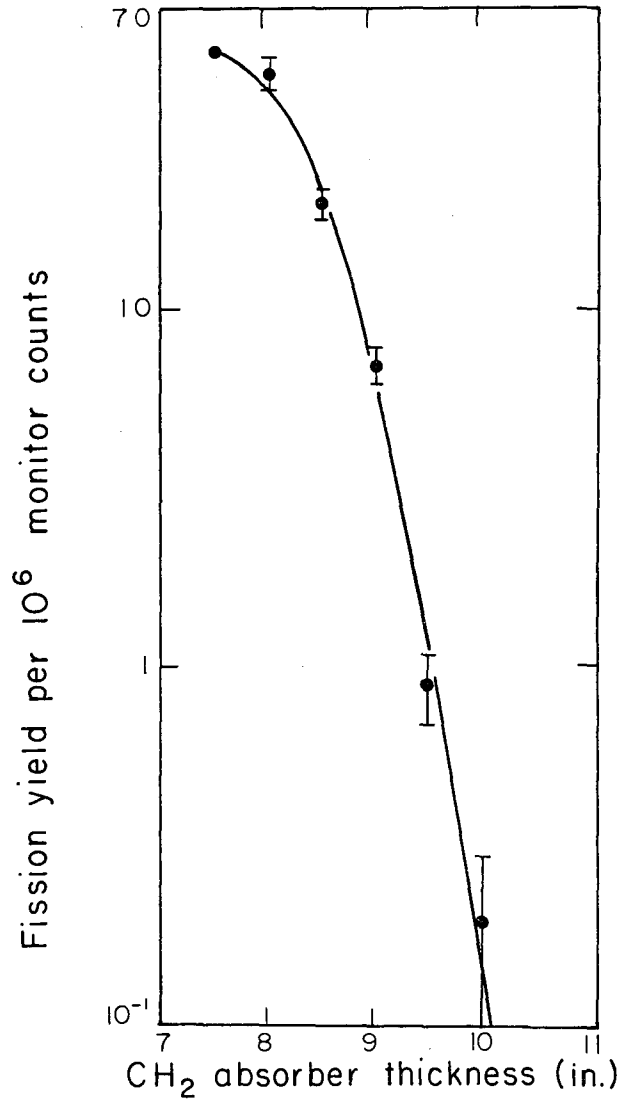
Fig. 5. Experimental arrangement.





MU-27150

Fig. 6. Differential range curve.



MU-27153

Fig. 7. Fission yield vs absorber thickness.

2. To determine the time scale, time calibration of the scope sweep was made every 3 h.

3. The stability of the fission discriminators was checked before and after every data run, to maintain the same fission-detection efficiency for each target throughout the experiment. In the case of  $\text{Th}^{232}$  and  $\text{U}^{238}$  the fission-detection efficiency was the same. This check was made by using a thin low-activity  $\text{Cf}^{252}$  source attached to the center plate of each of the targets. The activity of the source was known to better than 3%.

4. The zero-time of the time scale was determined with fissions from stopping  $\pi^-$  and it was done every 3 h. An accurate determination of the zero time was necessary to calculate the zero-time intercept of the time distribution of  $\mu$ -capture fission.

5. The actual data runs were 1 to 1-1/2 h long. Four to six runs were taken consecutively. The  $\text{Th}^{232}$ ,  $\text{U}^{238}$ , and  $\text{U}^{235}$  targets were alternated every 6 to 9 h. The background was measured simultaneously at negative times. The 7-msec beam spill of the 184-inch cyclotron was used, thus making the accidental rate almost negligible.

All through the data runs these parameters did not show any drift, and the original settings were not changed.

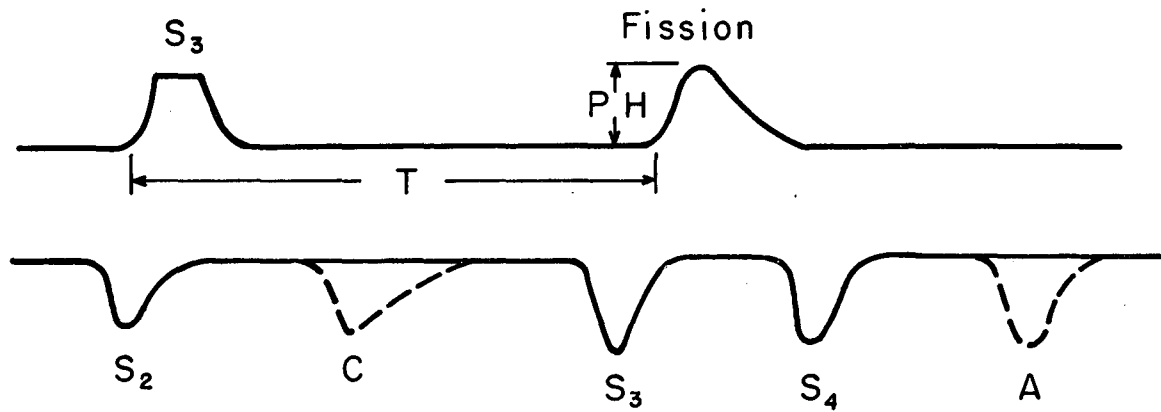
#### IV. DATA ANALYSIS

The film was scanned twice. In each event the fission-pulse height and its time relative to  $S_3$  were measured. The height of the fission pulse was measured from the top of the pulse to the straight parts of the sweep—always on the same edge of the trace. The time was measured from the point of maximum curvature at the leading edge of the  $S_3$  pulse to the same point in the fission pulse; these two points were well-defined. Figure 8 is a sketch of an event; the pulse height PH and the time T are indicated graphically. The presence of C and/or A counter pulses was noted, as well as the presence of pulses from counters  $S_3$  and  $S_4$  and their relative timing. (The film was read on a Recordak film reader.)

The criteria for an acceptable event were: (a) that no pulses from either counter C or A were present; (b) the fission-pulse height was larger than or equal to the minimum pulse height from a thin  $Cf^{252}$  source on the targets—this pulse height was called the unit pulse height; and (c) the relative timing of  $S_3$  and  $S_4$  was required to be the same as an absorber-out telescope event. Approximately 20% of the events did not fulfill the three criteria. The number of events for each target was 592 (Th), 1130 ( $U^{235}$ ), and 1328 ( $U^{238}$ ).

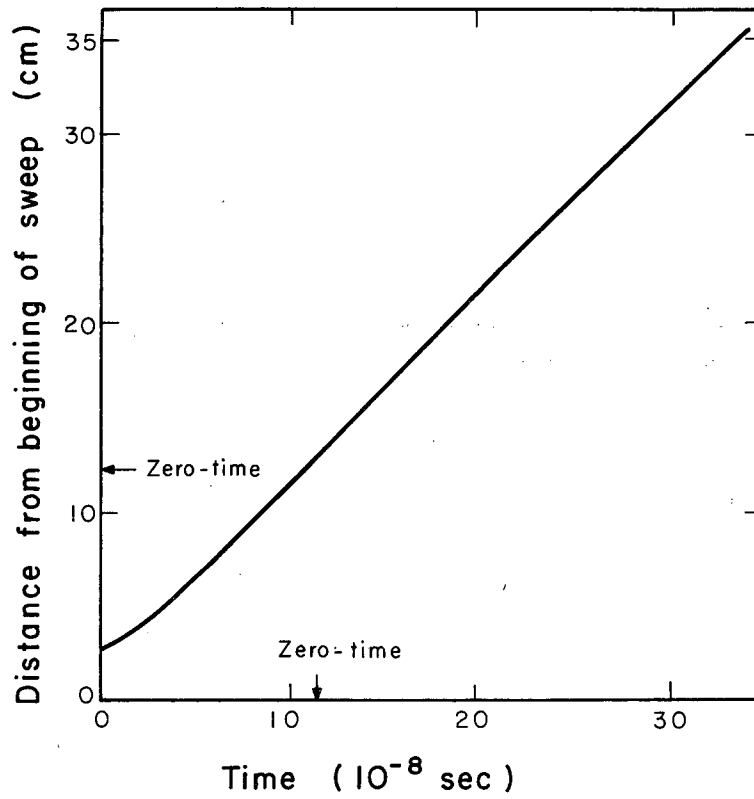
The time scale was obtained by counting the number of oscillations of the 50-Mc oscillator per unit length of the sweep. The time calibration was linear in the first 120 nsec and was nonlinear at times greater than 120 nsec. In the data analysis this nonlinearity was taken into consideration. Figure 9 shows a time calibration.

To obtain the zero-time intercept from  $\mu$ -capture fission-time distribution, we need to know the zero time accurately. The zero time was obtained from fissions produced by stopping  $\pi$ 's. Their time distribution is, for experimental purposes, a delta function at zero time. Due to the finite time resolution the delta-function time distribution appears Gaussian (see Fig. 10). This Gaussian distribution has a half-width of 1.5 nsec and introduces a significant modification on the exponential distribution of fission from  $\mu$  capture.



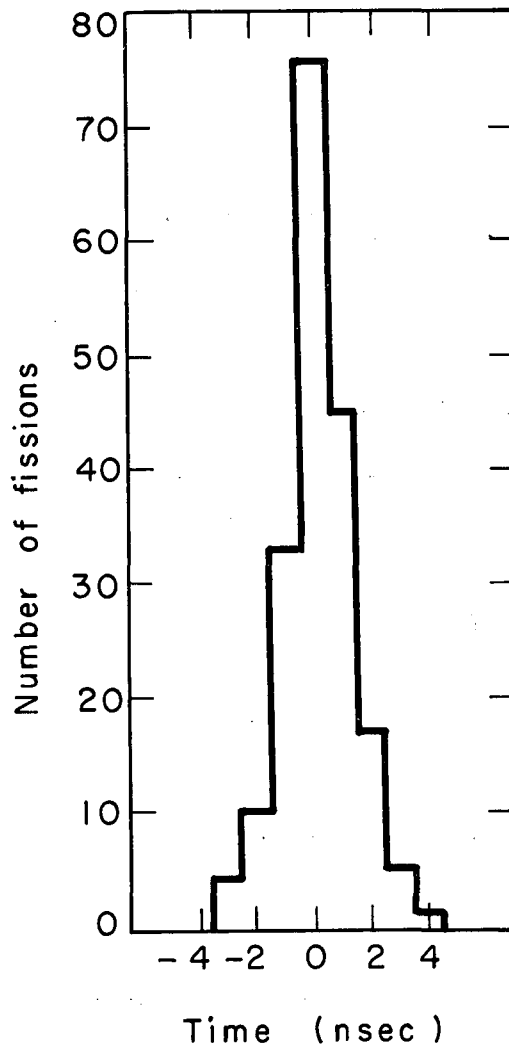
MU-27149

Fig. 8. Sketch of fission event on scope trace. (Dashed lines show the position of C and A, T is the time of fission pulse relative to  $S_3$ , and PH is the height of the fission pulse.)



MU-27145

Fig. 9. Time calibration of scope sweep.



MU-27207

Fig. 10. Zero time and time resolution determined with  $\pi$  fissions.

(Figure 11 shows the effect of the Gaussian distribution with  $\sigma = 1.5$  nsec on an exponential with a mean life of  $\tau = 75$  nsec. This effect was observed in the data, as can be seen from Fig. 12.) For this reason the events within the first 5 nsec at negative time were added to the first channel.

The data in  $U^{238}$  and  $U^{235}$  were divided approximately in equal parts and analyzed separately to obtain a consistency check on the results; then the data were added and analyzed as a whole. There were not sufficient data in  $Th^{232}$  to run this check. Table V shows the results of this consistency check.

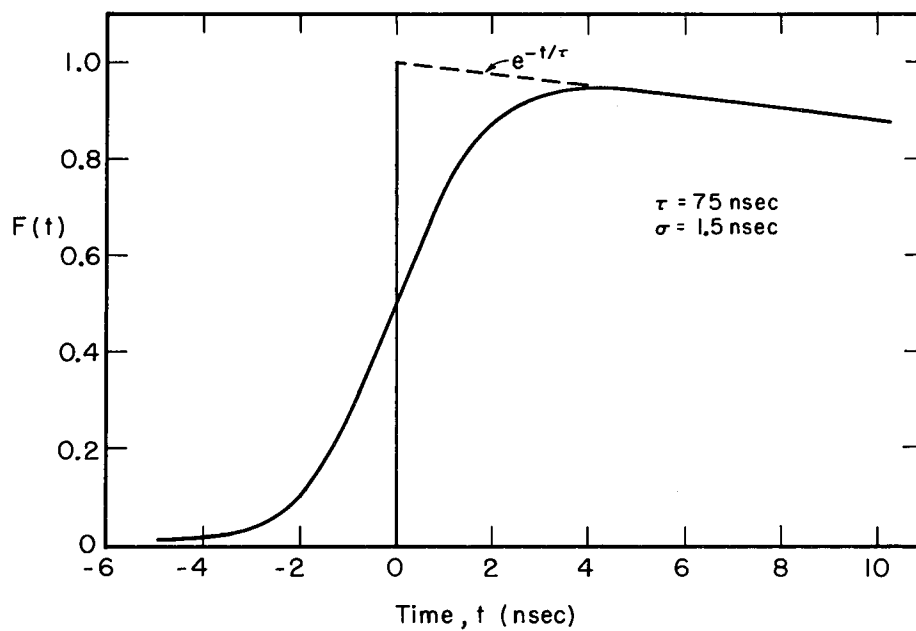
Table V. Comparison of results in  $U^{235}$  and  $U^{238}$  when the data were divided into two sections and analyzed independently.

Element		$\tau$ (nsec)	$I_0/10^{-8}\text{sec}^a$	<u>Excess in first channel</u> <u><math>\mu</math>-capture fission</u>
$U^{235}$	I	$67.0 \pm 5.6$	$66 \pm 6$	$12.6 \pm 3.2$
$U^{235}$	II	$63.9 \pm 6.3$	$83 \pm 10$	$9.5 \pm 3.2$
$U^{238}$	I	$73.2 \pm 3.8$	$88 \pm 5$	$5.8 \pm 2.1$
$U^{238}$	II	$75.3 \pm 5.2$	$91 \pm 7$	$8.6 \pm 1.7$

<sup>a</sup>  $I_0$ 's cannot be compared with each other, as the analysis was performed on a different number of events.

The scope sweep was linear from the measured zero time for 120 nsec; 1 cm of the sweep in this region was equivalent to 9.69 nsec. After this region the time equivalent of 1 cm of the sweep increased by 2% per cm. Only the first 190 nsec after zero-time was used in the data analysis. This is equivalent to approximately 2.8  $\mu$ -meson lifetimes in the target element. The data were divided into 19 channels approximately 10 nsec wide. In performing the least-squares fit the first channel was left out. The number of events per channel was converted into counts per  $10^{-8}$  sec and the best fit was obtained.

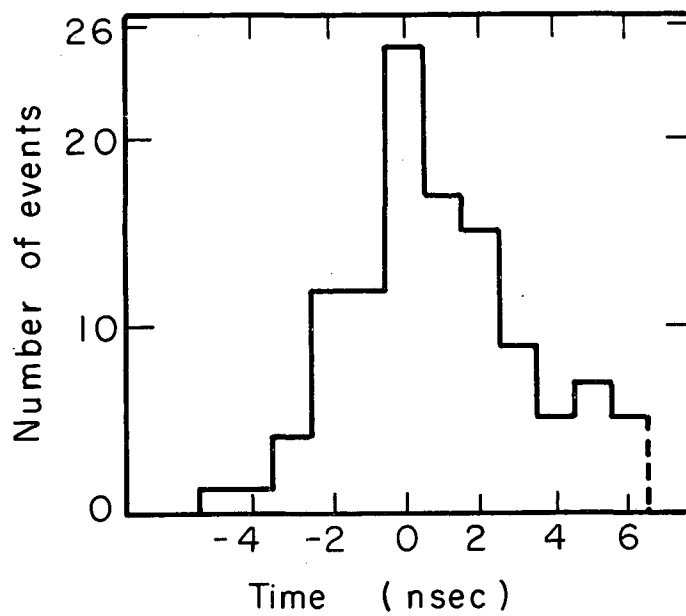




MU-25251

Fig 11. Effect of time resolution on exponential time distribution. The modified curve is described by

$$F(t) = \frac{\tau}{N_0} \frac{dN}{dt} = \exp(-t/\tau) \left[ \frac{1}{2} + \frac{1}{\sqrt{2\pi\sigma^2}} \int_{-t}^0 \exp(-y^2/2\sigma^2) dy \right].$$



MU-27152

Fig. 12. Sample of fissions produced by  $\mu^-$  in  $U^{238}$  to show effect of time resolution on the distribution of early-time events.

The least-squares fit to the data was made using Gauss' method and the IBM 704 program described in the LA-2367 report.<sup>45</sup> The program output gave the zero-time intercept and the mean life, with their standard errors. The background was changed by a standard deviation in both directions to study the sensitivity of our results to the background. The background changes produced a total change of 1.2% in the mean lives and negligible changes in the zero-time intercept. A  $\chi^2$  test was made on each fit as a measure of the validity of the fit. In all cases the  $P(\chi^2)$  was between 0.10 and 0.90. Figures 13, 14, and 15 show plots of the events vs time, and the best fits for the data. Table VI is a summary of the least-squares results.

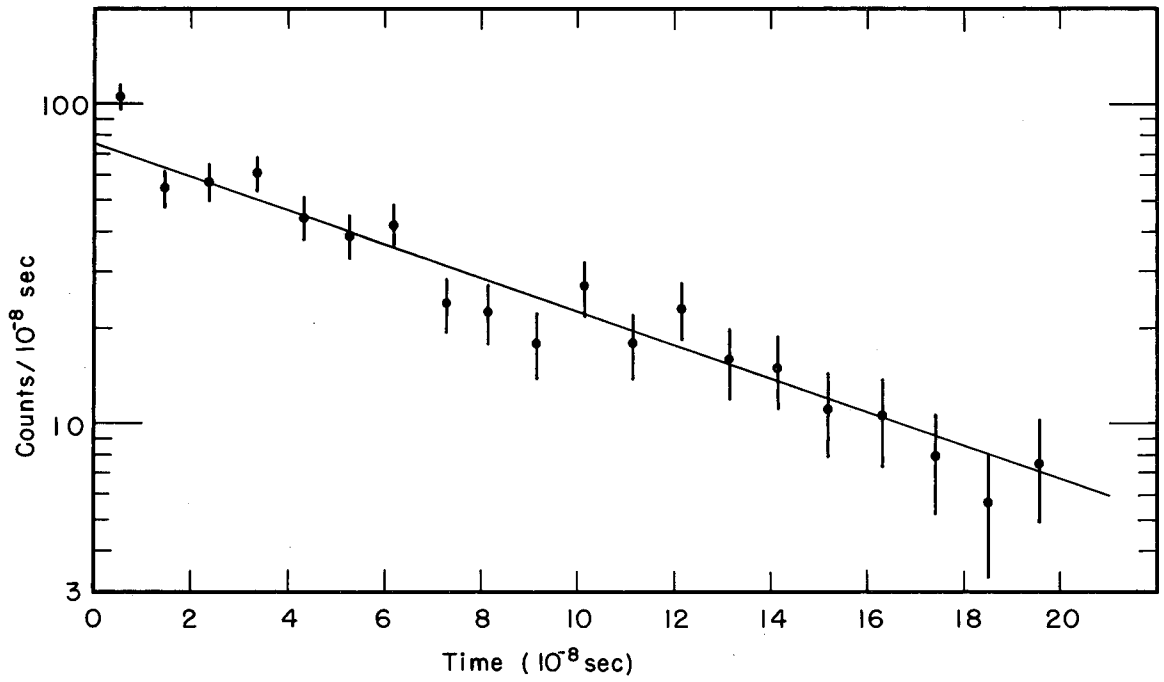
Table VI. Least-squares results for the Th<sup>232</sup>, U<sup>235</sup>, and U<sup>238</sup> Data.

Element	$\tau$ (nsec)	$I_0/10^{-8}$ sec	Background/ $10^{-8}$ sec
Th <sup>232</sup>	$74.2 \pm 5.6$	$74 \pm 6$	$1.87 \pm 0.56$
U <sup>235</sup>	$66.5 \pm 4.2$	$147 \pm 11$	$2.64 \pm 0.64$
U <sup>238</sup>	$75.6 \pm 2.9$	$179 \pm 7$	$0.32 \pm 0.32$

With this information we were able to calculate the contribution of  $\mu$ -capture fission in the first channel. Let  $I_0$  be the zero-time intercept and  $\tau$  the mean life; the contribution of  $\mu$ -capture fission in the first channel is given by

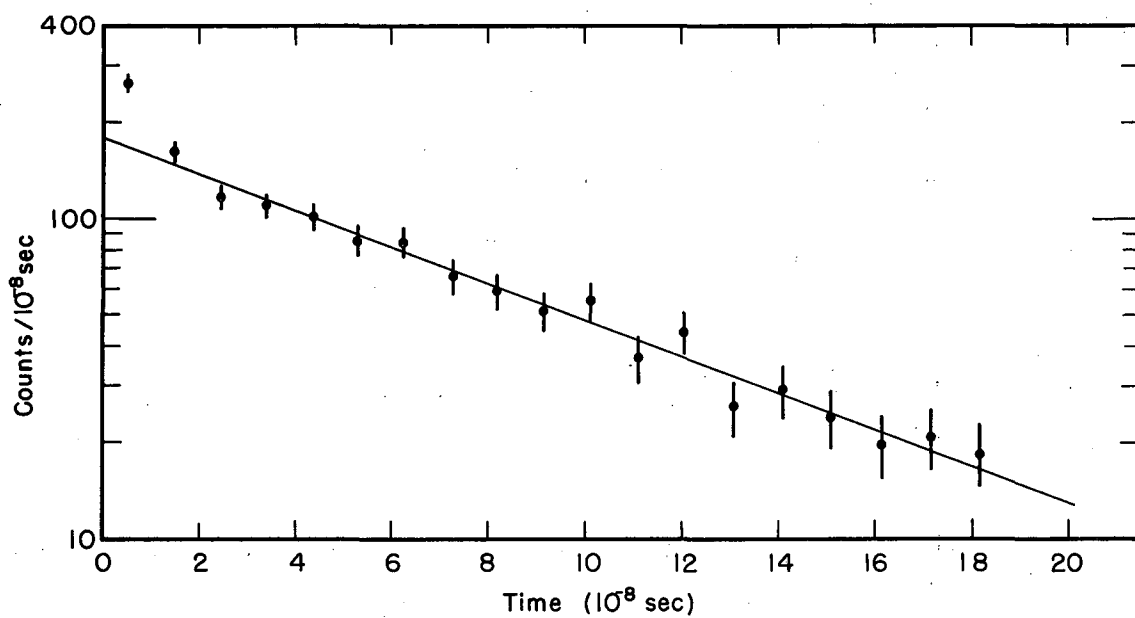
$$No_{cap} = I_0 \tau (1 - e^{-t_0/\tau}),$$

where  $t_0$  is the width of the first channel. The width of the first channel was measured from the time scale, and the zero time was determined by  $\pi^-$  fissions. The estimated error is less than 3% of the channel width. The error introduced into the calculated contribution of  $\mu^-$ -capture fission in this channel is a constant error. In all cases this error was very small compared with statistical error, and it is not



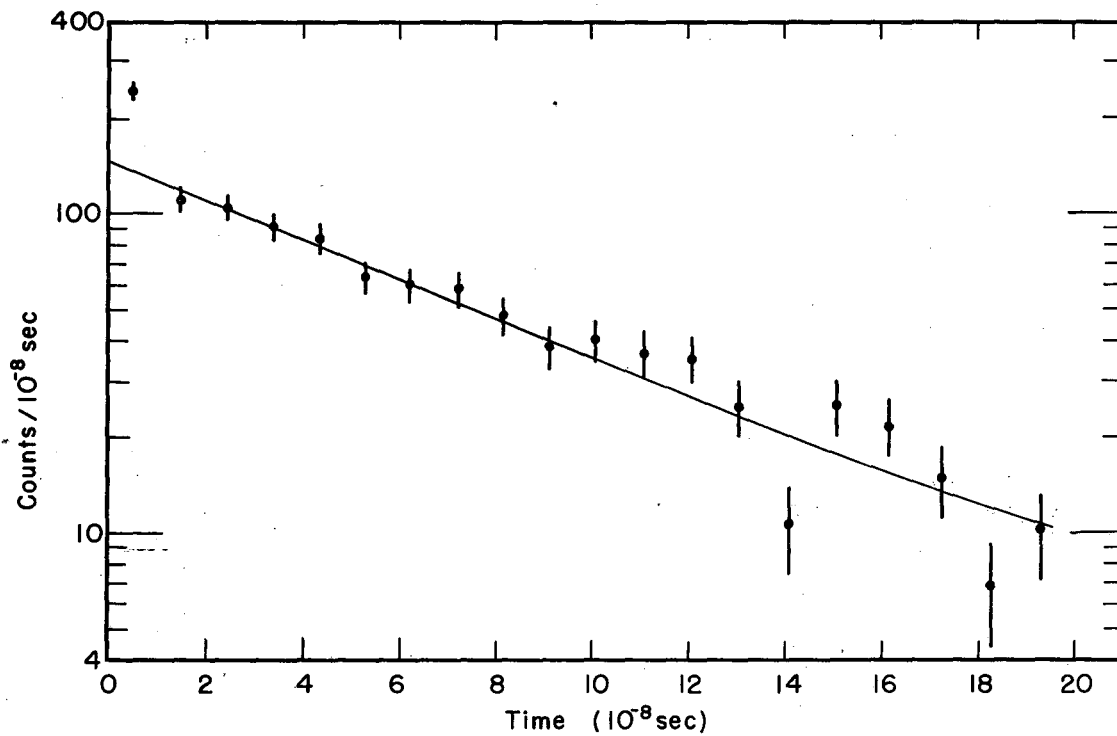
MU-25252

Fig. 13. Time distribution of the fissions of  $\text{Th}^{232}$  produced by  $\mu^+$ 's stopping in the target. The line is the best fit to the data when the first channel is not taken into consideration.)



MU-25254

Fig. 14. Time distribution of the fission of  $U^{238}$  produced by  $\mu^-$ 's stopping in the target. The line is the best fit to the data when the first channel is not taken into consideration.)



MU.25253

Fig. 15. Time distribution of the fissions of U<sup>235</sup> produced by  $\mu^-$ 's stopping in the target. The line is the best fit to the data when the first channel is not taken into consideration.)

included in the quoted error. The difference between the number of events in the first channel and the calculated contribution from  $\mu^-$ -capture fission gives the fission events associated with radiationless transition.

We did not determine the absolute stopping rate in the target because there was no reliable method to determine the effective target thickness in which fission can be detected. Therefore we did not obtain the fission probability associated with a stopping  $\mu$  meson. We express our results as the ratio of fissions associated with radiationless transition to fissions due to  $\mu^-$  capture. From our data we also obtained the ratio of  $\mu^-$  to  $\pi^-$  fission probability for all three targets. Table VII gives the results of the experiment.

Table VII: Results of the experiment

Element	$\frac{\text{Prompt fissions}}{\mu^- \text{ capture fission}}$	$\frac{\mu^- \text{ fission probability}}{\pi^- \text{ fission probability}}$
Th <sup>232</sup>	0.064 ± 0.022	0.085 ± 0.004
U <sup>238</sup>	0.072 ± 0.014	0.174 ± 0.007
U <sup>235</sup>	0.111 ± 0.021	0.281 ± 0.015

We have estimated the  $\pi^-$  contamination in our beam to be less than 0.1%. A further check on  $\pi^-$  contamination can be obtained by calculating the contamination that would be necessary to account for our results. If all prompt fissions are produced by  $\pi^-$ 's, then the  $\pi^-$  contamination would be given by

$$\frac{\mu^- \text{ fission probability}}{\pi^- \text{ fission probability}} \times \frac{\text{prompt fissions}}{\mu^- \text{ capture fissions}} = \frac{\pi^-}{\mu^-} \text{ stopping in the target.}$$

The targets were run at the same absorber thickness so one would expect the same  $\pi^-$  contamination in all three targets. Instead we find that the ratio is different for each target (see Table VIII), which indicates that our results cannot be explained by some anomalously large  $\pi^-$  contamination.

Table VIII. Summary of estimates of  $\pi^-$  contamination.

Element	$\pi^-$ contamination necessary to explain experimental results.	Zero-time excess due to estimated $\pi^-$ contamination $0.001 \pi^-/\mu^-$ .
Th <sup>232</sup>	0.0068	0.0093
U <sup>235</sup>	0.0318	0.0057
U <sup>238</sup>	0.0125	0.0036



## V. DISCUSSION AND CONCLUSIONS

To be able to reach any conclusions from the results of the experiment one must be able to ascertain that the excess prompt fission is not due to  $\pi^-$  contamination. The  $\pi^-$  contamination was discussed in Secs. IIA and IV. In summary we have: (a) From the range curve and the fission yield as a function of absorber thickness, the  $\pi^-$  contamination was less than 0.1%. With this  $\pi^-$  contamination one cannot account for the excess prompt fission, and its contribution is smaller than the statistical error of the results in all three targets. (b) We have also shown that the  $\pi^-$  contamination required to account for our results is different for the different targets, even though one expects the  $\pi^-$  contamination to be the same in all three targets because they were placed at the same absorber thickness (see Table VII). Since  $\pi^-$  contamination does not account for our results, we may conclude that the excess prompt fissions detected, while not produced by  $\mu^-$  capture, are due to stopping  $\mu$  mesons.

The proposed mechanism, by which the 2P-1S  $\mu$ -mesic atom transition transfers the quantum of energy to the nucleus, would produce prompt fission and give at least a qualitative explanation of our results. Also, this mechanism explains the results of the x-ray yield measurement of Mukhin et al.<sup>1</sup> There is no reliable way to calculate the probability of such radiationless transition because the nuclear wave functions are not known.

One may estimate the expected fraction of prompt fissions by using the fraction of x rays missing as the probability of radiationless transition and the measured photofission probability at 6.5 MeV (the 2P-1S transition energy is approximately 6.3 MeV). This estimate is valid provided the photoexcitation at this energy proceeds by the absorption of an electric dipole photon (see the Appendix).

We have calculated the prompt-fission yield as follows. We took the probability of radiationless transition to be the fraction of K x ray missing in  $U^{238}$  and  $Th^{232}$ , as measured by Mukhin et al.<sup>1</sup> The probability of fission at the energy of excitation produced by radiationless

transitions was taken to be the fission due to 6.5-MeV  $\gamma$ -rays [ $\sigma_f/(\sigma_f + \sigma_n) = 0.24$  in  $U^{238}$  and  $0.18$  in  $Th^{232}$ , where  $\sigma_f$  is the photo-fission cross section and  $\sigma_n$  is the neutron-emission cross section<sup>38</sup>].

We assume that the photoexcitation is produced by an electric dipole absorption, on the basis that the quadrupole photoexcitation with lower x-ray energies is negligible, as indicated by the data of Baz et al.<sup>47</sup> and Katz et al.<sup>48</sup> The product of the radiationless-transition probability and the photofission probability gives the probability of prompt fission associated with a stopping  $\mu$  meson. The results are given in Table IX. We also include in this table the ratio of expected prompt fissions to fissions produced by stopping  $\mu$  mesons, as measured with emulsions.<sup>49</sup>

Table IX. Summary of estimates of  $\pi^-$  contamination.

Element	(a) $\mu^-$ fission probability <sup>a</sup>	(b) Photofission probability at 6.5 MeV <sup>c</sup>	(c) Fraction of x ray missing <sup>d</sup>	(d)=(b)X(c) Fraction of $\mu^-$ expected to produce prompt fission	Prompt <sup>e</sup> fission total fis- sion
$Th^{232}$	$0.018 \pm 0.012^b$	0.18	0.15	0.027	1.50
$U^{238}$	$0.070 \pm 0.008$	0.24	0.23	0.055	0.79

<sup>a</sup> See reference 49.

<sup>b</sup> This value has very large error,  $\pm 0.012$ , therefore the results may not be reliable.

<sup>c</sup> See reference 38.

<sup>d</sup> See reference 1.

<sup>e</sup> Compare these results with those in Table VII.

Our results are smaller than expected, even when one reduces the dipole contribution to the photoexcitation to 50% in these targets. To explain the results one has to propose: (a) that there exists some other mechanism for radiationless transition beside the mechanism proposed by Zaretsky,<sup>2</sup> or the existence of a metastable state in the  $\mu$ -mesic atoms does not allow the  $\mu$  to reach the 1S state promptly, or (b) the Zaretsky mechanism is the one by which the  $\mu$  meson reaches the 1S, and the presence of the  $\mu$  meson in the 1S state modifies the fission process by increasing the fission barrier. There is no known mechanism besides Auger transition for a radiationless transition and it is negligible in high-Z mesic atoms for 2P-1S transitions. Also, there is no known metastable state in high-Z mesic atoms—the 2S state is higher than the 2P state due to the finite nuclear size.

The effect of the  $\mu^-$  in the 1S state on the fission process can be visualized as follows. In the liquid-drop model the stability against fission is determined by the change in the difference between the nuclear surface energy  $E_S$  and the Coulomb energy  $E_C$  when the nucleus deforms. The nucleus is stable if the change in  $(E_S - E_C)$  is positive, unstable if it is negative. Consider the deformation of a spherical nucleus of radius  $R$  into an ellipsoid: if  $a$  is the parameter that measures the extent of the deformation then

$$E_S = 0.014A^{2/3} \left[ 1 + \left( \frac{2}{5} \times a^2 \right) \right]$$

and

$$E_C = 0.000627 \left( \frac{Z^2}{A^{1/3}} \right) \left[ 1 - \left( \frac{1}{5} \times a^2 \right) \right].$$

The total change is then

$$a^2 \left[ \left( \frac{2}{5} \times 0.014 A^{2/3} \right) - \left( \frac{1}{5} \times 0.00067 \frac{Z^2}{A^{1/3}} \right) \right],$$

where  $A$  and  $Z$  are the mass and charge of the nucleus, respectively.

The  $\mu^-$  meson in 1S state spends approximately 50% of its time inside the nucleus in elements near U. This is equivalent to introducing negative charge into the nucleus or a decrease in Z, which would tend to make the change in potential energy less negative. Therefore a higher excitation energy would be required to produce fission, and this may be interpreted as an increase in the fission barrier. Zaretsky and Novikov have calculated the increase in the fission barrier due to the presence of the  $\mu^-$  meson.<sup>36</sup> They find that the increase is sufficient to raise the barrier to an energy approximately equal to the energy of the 2P-1S transition in  $U^{238}$ . From their results one may expect a considerable decrease in the fission probability (this is in agreement with our results). The order of magnitude in the change of the fission time due to changes in the height of the fission barrier may be estimated by using the relationship derived by Frankel and Metropolis<sup>50</sup> for the fission time for spontaneous fission:

$$T = 10^{-21} \times 10^{7.85 E_{th}},$$

where  $E_{th}$  is the height of the fission barrier (in MeV) and  $10^{-21}$  is the characteristic time associated with fissions over the barrier. This expression gives a change of a factor of ten in the fission time for every 0.13-MeV change in the fission barrier. From the calculations of Zaretsky, the presence of  $\mu^-$  mesons in the 1S state sets the fission barrier approximately 0.1 MeV above the 2P-1S transition energy in  $U^{238}$ . The fission probability in  $U^{238}$  would decrease by approximately a factor of ten, if we assume that the change in the fission time per change on the height of the fission barrier holds for any fission below the barrier, and if we take into consideration that the neutron emission time remains constant ( $\approx 10^{-21}$  sec). Our results indicate a change of this order in the fission probability.

In summary, our conclusions are: (a) evidence has been found for nuclear excitation associated with a stopping  $\mu^-$  meson that cannot be attributed to  $\mu^-$  nuclear capture, (b) such nuclear excitation can be

explained by 2P-1S radiationless transition as described by Zaretsky, and (c) the presence of the  $\mu^-$  meson in a 1S state of the mesic atom increases the fission barrier.

### ACKNOWLEDGMENTS

I wish to thank Dr. Selig Kaplan and Dr. Robert Pyle for their help and constant counsel in the performance and analysis of this experiment, and without whose help I could not have carried it to an end. Also, I wish to thank Professor Burton J. Moyer for his guidance and his interest in my work throughout my years of graduate study.

This work was done under the auspices of the U. S. Atomic Energy Commission.

## APPENDIX

The order of the multipole excitation<sup>45</sup> may be deduced from the angular distribution of the fission fragments. There are several measurements of the angular distribution in  $U^{238}$  and  $Th^{232}$  in the energy region from 6.5 to 14 MeV by L. Katz et al.<sup>47</sup> and A.I. Baz et al.<sup>48</sup> These experiments were done with a bremsstrahlung spectrum, and the energies quoted are the maximum energy of the spectrum.

To fit the angular distributions measured by Katz et al. requires an angular distribution of the form

$$I(\theta) = a + b \sin^2 \theta.$$

This is the angular distribution that would be expected from a dipole excitation. Although the results do not rule out a quadrupole excitation, we need not invoke any other but dipole excitation to explain these results.

The results of Baz et al. require an angular distribution of the form.

$$I(\theta) = a + b \sin^2 \theta + C \sin^2 \theta \cos^2 \theta,$$

which indicates that there is quadrupole as well as dipole excitation. At 6.5 MeV, his results give  $c/b = 0.75 \pm 0.71$ . From these results one may deduce the ratio of the quadrupole-to-dipole excitation cross section which produces fission:

$$\sigma_{fq}/\sigma_{fd} = 0.15 \pm 0.14.$$

The quadrupole contribution is very small and consistent with zero within a standard deviation. The Baz results show that the quadrupole contribution is very large at

$$E_{\max} = 9.4 \text{ MeV, which gives } \sigma_{fq}/\sigma_{fd} \approx 0.50.$$

Also, the results point to a decrease in the quadrupole contribution as the excitation energy approaches the threshold.

The information available on the angular distribution of fission fragments indicates that the quadrupole contribution to photoexcitation at energies below 7 MeV is very small or nonexistent. Therefore we may assume that the photoexcitation at 6.5 MeV proceeds by dipole absorption.

REFERENCES

1. M. B. Stearns and M. Stearns, *Phys. Rev.* 105, 1573 (1957); J. L. Lathrop, R. A. Lundy, V. L. Telegdi, and R. Winston, *Phys. Rev. Letters* 7, 147 (1961); A. I. Mukhin, M. J. Balatz, L. N. Kondratiev, L. G. Landsberg, P. I. Lebedev, Yu. V. Obukhov, and B. Pontecorvo, in Proceedings of the 1960 Annual International Conference on High-Energy Physics at Rochester (Interscience Publishers, Inc., New York, 1960), p. 550; E. P. Hincks, C. S. Johnson, and H. L. Anderson, Abstract, 1960, Canadian Association of Physicists Congress in Kingston, Canada.
2. D. F. Zaretsky, in Proceedings of the Second United Nations International Conference on the Peaceful Uses of Atomic Energy, (CERN, Geneva, 1958), Vol. 15, p. 175.
3. T. Kinoshita and A. Sirlin, *Phys. Rev.* 108, 844 (1957).
4. Hans Kruger, Momentum Dependence of the Asymmetry in Muon Decay (Ph. D. Thesis), Lawrence Radiation Laboratory Report UCRL-9322, Feb. 1961 (unpublished).
5. M. Bardon, P. Franzini, and J. Lee, *Phys. Rev. Letters* 7, 23 (1961).
6. P. C. Macq, K. M. Crowe, and R. P. Haddock, *Phys. Rev.* 112, 2061 (1958).
7. The value quoted is the weighted mean of the measurements of A. Astbury, P. M. Hattersley, M. Hussain, A. Kemp, and H. Muirhead, in Proceedings of the 1960 Annual International Conference on High-Energy Physics at Rochester (Interscience Publishers, Inc., New York, 1960), p. 542; J. Fischer, B. Leontre, A. Lundby, R. Meunier, and J. P. Stroot, *Phys. Rev. Letters* 3, 349 (1959); R. A. Reiter, T. A. Romanowski, R. B. Sutton, and B. G. Chidley, *Phys. Rev. Letters* 5, 22 (1960); V. L. Telegdi, in Proceedings of the 1960 Annual International Conference on High-Energy Physics at Rochester (Interscience Publishers, Inc., New York, 1960), p. 713.



8. T. Kinoshita and A. Sirlin, Phys. Rev. 113, 1962 (1959).
9. J. Sens, Phys. Rev. 113, 679 (1959).
10. H. Primakoff, Revs. Modern Phys. 31, 802 (1959).
11. M. L. Goldberger and S. B. Treiman, Phys. Rev. 111, 354 (1958).
12. R. P. Feynman and M. Gell-Mann, Phys. Rev. 112, 968 (1958).
13. N. F. Baker and C. Rubbia, Phys. Rev. Letters 3, 179 (1959).
14. A. Astbury, I. M. Blair, M. Hussein, A. Kemp, H. Muirhead, and R. G. P. Voss, Phys. Rev. Letters 3, 476 (1959). The latest measurement for  $\alpha$  is equal to  $-0.22 \pm 0.07$ —by A. Astbury, J. H. Bartley, I. M. Blair, N. A. R. Kemp, H. Muirhead, and T. Woodhead, University of Liverpool, Department of Physics Report (unpublished).
15. V. L. Telegdi, in Proceedings of the 1960 Annual International Conference on High-Energy Physics at Rochester (Interscience Publishers, Inc., New York, 1960), p. 713.
16. G. Culligan, J. F. Lathrop, V. L. Telegdi, R. Winston, and R. A. Lundy, Phys. Rev. Letters 7, 458 (1961).
17. R. H. Hildebrand, Phys. Rev. Letters 8, 34 (1962).
18. G. Charpak, F. J. M. Farley, R. L. Garwin, T. Muller, J. C. Sens, V. L. Telegdi, and A. Zichichi, Phys. Rev. Letters 6, 128 (1961).
19. G. Schrank, Princeton-Pennsylvania Accelerator Report PPAD-304D (unpublished).
20. J. L. Lloyd and A. W. Wolfendale, Proc. Phys. Soc. (London) A68, 1045 (1955).
21. D. Heggie, Y. Kim, G. Masek, and R. Williams, in Proceedings of the 1960 Annual International Conference on High-Energy Physics at Rochester (Interscience Publishers, Inc., New York, 1960), p. 793.
22. M. Conversi, E. Pancini, and O. Piccioni, Phys. Rev. 71, 209 (1947).
23. J. A. Wheeler, Revs. Modern Phys. 21, 133 (1949).
24. H. Ticho, Phys. Rev. 74, 1337 (1948).
25. F. D. S. Butement, Phil. Mag. 44, 208 (1953).
26. V. L. Fitch and Rainwater, Phys. Rev. 92, 789 (1953).

27. K. W. Ford and J. G. Wills, Los Alamos Scientific Laboratory of the University of California Report LAMS-2387, March 1960 (unpublished).
28. D. L. Hill and K. W. Ford, Phys. Rev. 94, 1617 (1953).
29. A. Devons, G. Gidal, M. L. Lederman, and G. Shapiro, in Proceedings of 1960 Annual International Conference on High-Energy Physics at Rochester (Interscience Publishers, Inc., New York, 1960), p. 785.
30. E. Fermi and E. Teller, Phys. Rev. 71, 209 (1947).
31. G. R. Burbidge and A. H. de Borde, Phys. Rev. 89, 189 (1953).
32. M. A. Ruderman, Phys. Rev. 118, 1632 (1960).
33. Values quoted in the American Institute of Physics Handbook, edited by D. E. Gray (McGraw-Hill Book Company, Inc., New York, 1957).
34. H. W. Koch, J. McElhinney, and E. L. Gasteiger, Phys. Rev. 77, 329 (1950).
35. E. K. Hyde, A Review of Nuclear Fission: Part One - Fission Phenomena at Low Energy, Lawrence Radiation Laboratory Report UCRL-9036, Jan. 1960 (unpublished).
36. D. F. Zaretsky and V. M. Novikov, Nuclear Phys. 28, 177 (1961).
37. R. A. Schmitt and R. B. Duffield, Phys. Rev. 105, 1277 (1957).
38. L. E. Lazareva, B. I. Gavrilov, B. N. Valuev, G. N. Zapsedina, and V. S. Stavinsky, Akademii Nauk S. S. S. R., in Conference of the Academy of Sciences on Peaceful Uses of Atomic Energy, 1955 (Consultants Bureau, New York, 1955), p. 306.
39. H. A. Bethe, Revs. Modern Phys. 9, 69 (1937).
40. S. N. Kaplan, B. J. Moyer, and R. V. Pyle, Phys. Rev. 112, 968 (1958).
41. C. S. Johnson, E. P. Hincks, and H. L. Anderson, Bull. Am. Phys. Soc. 5, 369 (1960).
42. Harry Bowman (Lawrence Radiation Laboratory, Berkeley) private communication.
43. R. Swanson, private communication through Dr. Selig Kaplan.

44. R. K. Symon, Fluctuations in Energy Loss by High-Energy Charged Particles in Passing Through Matter (Ph. D. Thesis), Harvard University, Jan. 1948 (unpublished).
45. R. H. Moore and R. K. Zeigler, Los Alamos Scientific Laboratory of the University of California Report LA-2367, March 1960 (unpublished).
46. J. J. Griffin, Phys. Rev. 116, 107 (1959).
47. L. Katz, A. P. Baerg, and F. Brown, in Proceedings of the Second United Nations International Conference on the Peaceful Uses of Atomic Energy (CERN, Geneva 1958), Vol. 15, p. 188.
48. A. I. Baz, N. M. Kulikova, L. E. Lazareva, N. V. Nikitina, and V. A. Semenov, in Proceedings of the Second United Nations International Conference on the Peaceful Uses of Atomic Energy (CERN, Geneva, 1958), Vol. 15, p. 184.
49. M. G. Petrashku and A. K. Mikhul, Soviet Phys. -Doklady 4, 628 (1959) give  $\mu^-$  fission probability in  $\text{Th}^{232}$ , and the same authors in Soviet Phys. -Doklady 4, 92 (1959) give the  $\mu^-$  fission probability in  $\text{U}^{238}$ .
50. S. Frankel and N. Metropolis, Phys. Rev. 72, 914 (1947).

This report was prepared as an account of Government sponsored work. Neither the United States, nor the Commission, nor any person acting on behalf of the Commission:

- A. Makes any warranty or representation, expressed or implied, with respect to the accuracy, completeness, or usefulness of the information contained in this report, or that the use of any information, apparatus, method, or process disclosed in this report may not infringe privately owned rights; or
- B. Assumes any liabilities with respect to the use of, or for damages resulting from the use of any information, apparatus, method, or process disclosed in this report.

As used in the above, "person acting on behalf of the Commission" includes any employee or contractor of the Commission, or employee of such contractor, to the extent that such employee or contractor of the Commission, or employee of such contractor prepares, disseminates, or provides access to, any information pursuant to his employment or contract with the Commission, or his employment with such contractor.

